Published in final edited form as:
Biomaterials. 2012 May ; 33(13): 3503–3514. doi:10.1016/j.biomaterials.2012.01.041.

The effect of oxidation on the degradation of photocrosslinkable alginate hydrogels

Oju Jeon[a], **Daniel S. Alt**[a], **Shaoly M. Ahmed**[a], and **Eben Alsberg**[a,b,*]

[a]Department of Biomedical Engineering, Case Western Reserve University, Cleveland OH 44106, USA

[b]Department of Orthopaedic Surgery, Case Western Reserve University, Cleveland OH 44106, USA

Abstract

Recently, we reported on a new photocrosslinkable alginate-based hydrogel, which has controllable physical and cell adhesive properties. The macromer solution containing cells can be injected in a minimally invasive manner into a defect site and crosslinked while maintaining high cell viability. The number of hydrolyzable ester bonds in the formed crosslinks may be controlled by altering the degree of methacrylation on the alginate polymer backbone. However, the degradation rate of the hydrogels has been found to be slower in vivo than in vitro. The purpose of this study was to develop photocrosslinked alginate hydrogels with an increased range of biodegradation rates for more rapid in vivo biodegradation in regenerative medicine and bioactive factor delivery applications. Therefore, we oxidized alginate prior to methacrylation to change the uronate residue conformations to an open-chain adduct, which makes it more vulnerable to hydrolysis. Here, we demonstrate that the swelling behavior, degradation profiles, and storage moduli of photocrosslinked hydrogels formed from oxidized, methacrylated alginates (OMAs) are tunable by varying the degree of alginate oxidation. The OMA macromers and photocrosslinked OMA hydrogels exhibited cytocompatibility when cultured with human bone marrow-derived mesenchymal stem cells (hBMMSCs). In addition, hMSCs derived from bone marrow or adipose tissue photoencapsulated within these hydrogels remained viable, and their proliferation rate was a function of alginate oxidation level and initial hydrogel weight fraction. Oxidation permits a wider range of photocrosslinked OMA hydrogels physical properties, which may enhance these therapeutic materials' utility in tissue engineering and other biomedical applications.

Keywords

Biodegradation; Biomaterials; Mesenchymal stem cells; Tissue engineering

1. Introduction

Recently, we developed alginate macromers that can be photopolymerized to form hydrogels with controllable mechanical properties, swelling ratios, and degradation rates in vitro [1]. Cells could be easily encapsulated via suspension in aqueous macromer solution followed by in situ photocrosslinking, and the resultant hydrogels showed excellent cytocompatibility. We have also demonstrated the capacity to control the cell adhesivity of these hydrogels by covalently coupling cell adhesion ligands, such as those containing the

[*]Corresponding author. Department of Biomedical Engineering, Case Western Reserve University, Cleveland OH 44106, USA. Tel.: +1 216 368 6425; fax: +1 216 368 4969. eben.alsberg@case.edu (E. Alsberg).

RGD sequence, to the methacrylated alginate backbone [2]. RGD modification of photocrosslinked alginate hydrogels promoted cell adhesion and spreading on the surface of the photocrosslinked alginate hydrogels, and enhanced the proliferation of encapsulated cells. Additionally, we presented an affinity-based growth factor delivery system using photocrosslinked alginate hydrogels by incorporation of methacrylated heparin, which can be coupled to alginate hydrogels through photopolymerization, to allow for the controlled and prolonged release of heparin binding growth factors, such as fibroblast growth factor-2, vascular endothelial cell growth factor, transforming growth factor-β_1, and bone morphogenetic protein-2. The release profiles of growth factors from the heparin-modified hydrogels were sustained over three weeks with no initial burst release, and the released growth factors retained their biological activity [3]. The implantation of growth factor-laden hydrogels in an animal model resulted in enhanced new tissue formation, however, the degradation rate of these hydrogels was found to be much slower in media than in water and in vivo than in vitro, limiting new tissue formation in the hydrogels [3].

Since alginate is not naturally enzymatically degraded in mammals, ionically crosslinked alginate hydrogels exhibit a remarkably slow degradation rate, which is typically months to years for their complete removal from injection sites [4,5]. Thus, the degradation kinetics of alginate hydrogels has been previously controlled, for example, by varying alginate molecular weight [6] and incorporation of biodegradable crosslinks [1]. In another approach, oxidized alginates (OAs) were synthesized to accelerate the degradation rate of alginate [7–11]. When alginate is oxidized by reacting with sodium periodate, the carbon–carbon bonds of the *cis*-diol groups in the uronate residues are cleaved [7,10] and changed to dialdehyde groups. This approach offers control over the degradation rate by varying the oxidation degree, as increasing the oxidation degree can increase the vulnerability of alginate hydrogels to hydrolysis [8,10].

The purpose of this study was to develop photocrosslinked alginate hydrogels with an increased range of biodegradation rates for more rapid in vivo biodegradation in tissue engineering and bioactive factor delivery applications. Therefore, we oxidized the alginate prior to methacrylation to change the uronate residue conformations to an open-chain adduct, which would be more prone to hydrolytic degradation [10]. In this manner, hydrolytic degradation could take place both at the alginate polymer backbone and at the ester bonds in the photopolymerized crosslinks [12]. In this study, we investigated whether the swelling behavior, degradation profiles, and storage moduli of photocrosslinked hydrogels formed from oxidized and methacrylated alginates (OMAs) are tunable by varying the degree of alginate oxidation. The potential applicability of these photocrosslinked OMA hydrogels as a carrier of human mesenchymal stem cells (hMSCs) derived from bone marrow and adipose tissue was also examined in vitro.

2. Materials and methods

2.1. Preparation of OA

The OA was prepared by reacting sodium alginate (Protanal LF 20/40, 196,000 g/mol, FMC Biopolymer, Philadelphia, PA, USA) with sodium periodate (Sigma) using a modification of a previously described method [10,13]. Briefly, sodium alginate (20 g) was dissolved in ultrapure deionized water (diH_2O, 1800 ml) overnight. Sodium periodate (2.0, 3.5, 5.0, and 10.1 g) was dissolved in 200 ml diH_2O and added into separate alginate solutions to achieve different degrees of theoretical alginate oxidation (10, 17.5, 25, and 50%, respectively) under stirring in the dark at room temperature (RT), and the reaction was stopped after 24 h by the addition of ethylene glycol (molar ratio of ethylene glycol:sodium periodate = 1:1). The OA was purified by dialysis (MWCO 3500; Spectrum Laboratories Inc., Rancho

Dominguez, CA, USA) against deionized ultra pure water (diH_2O) for 3 days, filtered (0.22 μm filter), and lyophilized.

2.2. Synthesis of OMA macromer

The OMA macromer was prepared by reacting OA with 2-aminoethyl methacrylate (AEMA, Sigma, St. Louis, MO, USA) [1,12]. To prepare OMA at a theoretical methacrylation of 45%, OA (10 g) was dissolved in a buffer solution (1w/v %, pH 6.5) of 50 mM 2-morpholinoethanesulfonic acid (MES, Sigma) containing 0.5 M NaCl. N-hydroxysuccinimide (NHS, 2.65 g; Sigma) and 1-ethyl-3-(3-dimethylaminopropyl)-carbodiimide hydrochloride (EDC, 8.75 g; Sigma) (molar ratio of NHS:EDC = 1:2) were added to the mixture to activate the carboxylic acid groups of the alginate. After 5 min, AEMA (3.8 g) (molar ratio of NHS:EDC:AEMA = 1:2:1) was added to the product, and the reaction was maintained in the dark at RT for 24 h. The reaction mixture was precipitated with the addition of excess of acetone, dried under reduced pressure, and rehydrated to a 1w/v % solution in diH_2O for further purification. The OMA was purified by dialysis against diH_2O (MWCO 3500; Spectrum Laboratories Inc.) for 3 days, treated with activated charcoal (0.5 mg/100 ml, 50–200 mesh, Fisher, Pittsburgh, PA) for 30 min, filtered (0.22 μm filter), and lyophilized.

2.3. Characterization of OMAs

The OMAs were dissolved in deuterium oxide (D_2O, 2 w/v %), and placed in an NMR tube. To analyze the oxidation and methacrylation efficiency of the OMAs, ^1H NMR spectra were recorded on a Varian Unity-300 (300 MHz) NMR spectrometer (Varian Inc., Palo Alto, CA, USA) using 3-(trimethylsilyl)propionic acid-d_4 sodium salt (0.05 w/v %) as an internal standard. The actual oxidation was determined from ^1H NMR spectra based on the ratio of the integrals for the methyl protons (Fig. 1B, a) to the newly formed methyl protons (Fig. 1B, a′) by oxidation of alginate. The actual alginate methacrylation was also calculated from ^1H NMR spectra based on the ratio of the integrals for the internal standard protons to the methyl (Fig. 1C, c) and methylene protons (Fig. 1C, b) of methacrylate. The actual oxidation was used in a naming code for the different alginate formulations (see Table 1). The weight average molecular weight of OMAs was measured by gel permeation chromatography (GPC, Waters, Milford, MA) using a Waters 2690 separations module equipped with size exclusion columns (Ultrahydrogel 500, Waters), refractometer (Waters 410), and UV detector (Waters 2487) [14].

2.4. Photocrosslinking OMA hydrogels

To fabricate photocrosslinked OMA hydrogels, OMA was dissolved in Dulbecco's Modified Eagle Medium with low glucose (DMEM, Sigma) with 0.05w/v % photo-initiator (Irgacure-2959, Sigma). The OMA solutions (2, 4, and 8 w/v %) were injected between two glass plates separated by 0.75 mm spacers and photocrosslinked with 365 nm UV light (Model EN-280L, Spectroline, Westbury, NY) at ~1 mW/cm^2 for 15 min to form the hydrogels. Photocrosslinked OMA hydrogel disks were created using an 8 mm diameter biopsy punch and placed in 15 ml conical tube containing 10 ml DMEM for 1 h for swelling and degradation studies, mechanical testing, and culture of cells on the hydrogel surfaces.

2.5. Swelling and degradation of photocrosslinked OMA hydrogels

The photocrosslinked OMA hydrogels were lyophilized and dry weights (W_i) were measured. Dried hydrogel samples were immersed in 50 ml of DMEM and incubated at 37 °C to reach equilibrium swelling state for 24 h. The DMEM was replaced every week. Over the course of 4 weeks, samples were removed, rinsed with DMEM, and the swollen (W_s) hydrogel sample weights were measured. The swelling ratio (Q) was calculated by $Q = W_s/$

W_i ($N = 3$ for each time point). After weighing the swollen hydrogel samples, the samples were lyophilized and weighed (W_d). The percent mass loss was calculated by $(W_i - W_d)/W_i \times 100$ ($N = 3$ for each time point).

2.6. Rheology

The rheological properties of the photocrosslinked OMA hydrogels were measured using a strain-controlled AR-2000ex rheometer (TA Instruments, New Castle, DE, USA) with stainless-steel parallel plate geometry (plate diameter of 8 mm, gap of 0.7–0.8 mm). At predetermined time points, swollen alginate hydrogel disks were punched once again to match the diameter of the parallel plates (8 mm). The measurement was performed using a dynamic frequency sweep test in which a sinusoidal shear strain of constant peak amplitude (0.1%) was applied over a range of frequencies (0.6–10 rad/s). The strain used was within the linear viscoelastic region, as determined by dynamic strain sweep experiments (up to 10% strain at 10 rad/s frequency).

2.7. Cytotoxicity tests of OMA macromers and photocrosslinked OMA hydrogels

To evaluate cytotoxicities of OMAs and photocrosslinked OMA hydrogels, an indirect contact methodology was employed. Briefly, a human bone marrow aspirate was harvested from the posterior iliac crest of a donor after informed consent under a protocol approved by the University Hospitals of Cleveland Institutional Review Board. The human bone marrow-derived mesenchymal stem cells (hBMMSCs) were isolated from the bone marrow aspirate and cultured in the Skeletal Research Center Mesenchymal Stem Cell Facility as previously described [15,16]. hBMMSCs (passage 2) were plated in 6-well plates at 1×10^5 cells/well in 3 ml of DMEM containing 10 v/v % fetal bovine serum (FBS, Sigma) and cultured at 37 °C and 5% CO_2 for 24 h. Cell culture inserts (25 mm in diameter, 8 μm pore size on PET track-etched membrane; Becton Dickinson Labware Europe, Le Pont De Claix, France) were placed into each well. Sterile OMA solution (1 ml, 2w/v % in DMEM) or a photocrosslinked OMA hydrogel (1 ml), which was made in a 48-well plate, was added into each culture insert ($N = 3$). hBMMSCs cultured with a cell culture insert but without the presence of any macromer or hydrogel material were maintained as a comparative group. A control group, not exposed to any chemicals or inserts, was maintained in parallel. After 48 h incubation, media, inserts, and hydrogels were removed. Each well was rinsed with Dulbecco's phosphate buffered saline (DPBS, Thermo Fisher Scientific Inc., Waltham, MA), and 3 ml of a 20% CellTiter 96 Aqueous One Solution (Promega Corp., Madison, WI, USA), which contains 3-[4,5-dimethylthiazol-2-yl]-5-[3-carboxymethoxy-phenyl]-2-[4-sulfophenyl]-2H-tetrazolium (MTS-tetrazolium) in DPBS was added to each well. The MTS-tetrazolium compound can be metabolized by mitochondria in living cells into a colored formazan product that is soluble in cell culture medium. After incubating at 37 °C for 90 min, the absorbance of the solutions was determined at 490 nm using a 96-well plate reader (SAFIRE, Tecan, Austria).

2.8. hBMMSC culture on photocrosslinked OMA hydrogels

hBMMSCs were seeded onto photocrosslinked OMA hydrogel disks in 24-well tissue culture plates in 1 ml DMEM containing 10% FBS at a seeding density of 1×10^4 cells/cm^2 and allowed to adhere at 37 °C with 5% CO_2 for 4 h ($N = 3$). The photocrosslinked OMA hydrogel disks were then transferred to new plates containing fresh media. After 4 h incubation, the number of adhered cell was quantified using three different fields of light microscopic images on the hydrogel disks ($N = 3$) taken using an ECLIPSE TE 300 microscope (Nikon, Tokyo, Japan) equipped with a digital camera (Retiga-SRV, Qimaging, Burnaby, BC, Canada).

The viability and morphology of adhered hBMMSCs on the photocrosslinked OMA hydrogels disks were examined using a Live/Dead assay comprised of fluorescein diacetate (FDA, Sigma) and ethidium bromide (EB, Sigma) [1]. After 7 days, 20 μl of staining solution was added into each well and incubated for 3–5 min at room temperature, and then stained hydrogel-cell constructs were imaged using fluorescence microscopy (ECLIPSE TE 300) equipped with a digital camera (Retiga-SRV).

2.9. Photoencapsulation of hMSCs

Human adipose tissue-derived mensenchymal stem cells (hADSCs) were isolated from the adipose tissue using a modification of a previous method [17]. Briefly, human adipose tissue was obtained by liposuction from informed and consenting patients. After the tissue was washed seven times with DPBS (Invitrogen, Carlsbad, CA, USA) to remove contaminating blood, adipose tissue was then digested in DPBS containing 1% bovine serum albumin (Invitrogen), 0.1% collagenase type I (Worthington Biochemical, Lakewood, NJ), and 2 mM calcium chloride (Sigma) for 40 min at 37 °C with gentle shaking. After floating adipocytes were removed from the stromal fraction by density centrifugation, hADSCs were cultured to P1 in DMEM/F-12 (BioWhittaker, Suwanee, GA) supplemented with 10% FBS (HyClone, Logan, UT), and 100 U/ml penicillin and 100 μg/ml streptomycin (BioWhittaker, Suwanee, GA, USA), and they were expanded to P2 in the aforementioned media supplemented with 10% FBS, 100 ng/ml recombinant human fibroblast growth factor-2 (R&D Systems, Minneapolis, MN). hBMMSCs or hADSCs at passage 2 were photoencapsulated in OMA hydrogels by suspension in OMA solution (2, 4, and 8w/v % in DMEM) with 0.05w/v % photoinitiator. The cell/macromer solutions (5×10^6 cells/ml) were injected between two glass plates separated by 0.75 mm spacers and photocrosslinked with 365 nm UV light at ~1 mW/cm^2 for 10 min to form the hydrogel-cell constructs. Photocrosslinked OMA hydrogel disks were created using a 6 mm diameter biopsy punch and placed in 24-well tissue culture plates with 1 ml of DMEM containing 10% FBS, and cultured in a humidified incubator at 37 °C with 5% CO_2 with gentle shaking for 4 weeks. The media was replaced every three days.

2.10. Assays of photoencapsulated hMSCs

The viability of encapsulated hBMMSCs and hADSCs in the photocrosslinked OMA hydrogels was investigated using the Live/Dead assay at predetermined time points as described earlier. The images were taken using fluorescence microscopy (ECLIPSE TE 300) equipped with a digital camera (Retiga-SRV) from three different fields in the center of cell/hydrogel constructs.

To investigate cell proliferation within the hydrogels, the DNA content of encapsulated hMSCs and hADSCs in photocrosslinked OMA hydrogels was quantified by using the Quant-iT™Picogreen®dsDNA assay (Invitrogen) according to the manufacturer's instruction. At each time point, hydrogel-cell constructs were removed from media, homogenized for 30 s using a TH homogenizer (Omni International, Marietta, GA) and digested in 1 ml papain buffer solution (25 μg/ml papain; Sigma, 2 mM L-cysteine; Sigma, 50 mM sodium phosphate; Sigma, 2 mM ethyl-enediaminetetraacetic acid; Fisher pH 6.5 in nuclease-free water; Ambion, Austin, TX) at 65 °C overnight. After centrifuging the papain-digested samples at 16200 g for 10 min, 100 μl of supernatant was mixed with 100 μl of 1 × TE buffer (Invitrogen) containing fluorescent PicoGreen® reagent and incubated at room temperature for 30 min. Fluorescence intensity of the dye-conjugated DNA solution was measured in 96-well plates on a plate reader (480 nm excitation and 520 nm emission, SAFIRE), and the DNA content was calculated from a standard curve generated with calf thymus DNA (Invitrogen).

2.11. Statistical analysis

All quantitative data is expressed as mean ± standard deviation. Statistical analysis was performed with one-way analysis of variance (ANOVA) with Tukey honestly significant difference post hoc test using Origin software (OriginLab Co., Northampton, MA). A value of $p < 0.05$ was considered statistically significant.

3. Results

3.1. Synthesis and characterization of OMA

To prepare photocrosslinkable OMA macromers, sodium alginates were oxidized using sodium periodate in aqueous solution at room temperature for 24 h, and then methacryl groups were introduced into the OA main chains as shown in Fig. 1A. The experimental efficiencies of alginate oxidation and methacrylation were calculated from ^{1}H NMR spectra. The ^{1}H NMR spectra of OAs and OMAs are shown in Fig. 1B and C, respectively. The ratio of sodium periodate to the number of alginate repeating units was varied to obtain different degrees of oxidation (Table 1). The theoretical oxidation of the hydroxyl groups on carbons 2 and 3 of the repeating units of alginate was varied from 10% to 50%. Increasing the theoretical oxidation of alginate from 10% to 50% resulted in an increase in the oxidation of alginate from 9% to 44%. The intensities of proton peaks of OMA (Fig. 1B, a′) increased as the actual oxidation of the alginate increased from 9% to 44%. The OAs were then methacrylated to a theoretical extent of 45% of the carboxyl groups using AEMA. Theoretical methacrylation was calculated on the basis of the concentration of AEMA added to the OA solution [1]. The ^{1}H NMR spectra of OMA exhibited peaks of vinyl methylene (Fig. 1C, b) and methyl (Fig. 1C, c) protons that were newly formed by the reaction with AEMA at δ6.2 and 5.7, and 1.9, respectively.

3.2. Swelling kinetics and degradation of OMA hydrogels

Photocrosslinked OMA hydrogels were prepared with different degrees of alginate oxidation and OMA macromer concentrations. The swelling ratio change of the hydrogels measured over time reflects changes in their physical and chemical structure. Swelling ratios of OMA-9 and OMA-14 with different weight percentages of OMA in DMEM are shown in Fig. 2A and B, respectively. The swelling of OMA-9 hydrogels decreased as the weight percentage of OMA in the hydrogels increased. All OMA-9 hydrogels reached equilibrium swelling within 7 days (Fig. 2A) and then stayed relatively constant for 4 weeks. Compared to the OMA-9, OMA-14 exhibited much faster swelling kinetics. The swelling of OMA-14 reached a maximum by day 1 (2 and 4 w/v %) or 1 week (8 w/v %) and then rapidly decreased as they degraded (Fig. 2B).

The mass loss (%) of OMA-9 and OMA-14 hydrogels over time was determined as a measure of degradation (Fig. 2C and D). OMA-9 hydrogels with different weight percentages of OMA had relatively similar degradation rates (Fig. 2C). Compared to OMA-9, OMA-14 hydrogels exhibited the faster degradation with complete degradation of three different conditions occurring between 1 and 3 weeks. As the weight percentage of alginate in OMA-14 hydrogels increased, their degradation rate decreased (Fig. 2D). All OMA-20 and OMA-44 hydrogels degraded too rapidly to measure swelling ratio and mass loss. OMA-20 (2 w/v %) and all OMA-44 (2, 4, and 8 w/v %) hydrogels were completely degraded within 12 h. OMA-20 hydrogels made with 4 and 8 w/v % were completely degraded by day 2 and day 3, respectively.

3.3. Rheological properties of the photocrosslinked OMA hydrogel

Dynamic mechanical analysis was performed by measuring the mechanical response of the OMA hydrogels (4 w/v %) with different degrees of alginate oxidation to deformation under

oscillatory strain to yield quantitative information on the viscoelastic and rheological properties of the hydrogels. The storage moduli (G') of OMA hydrogels are presented as a function of radial frequency. G' of the hydrogels exhibited a pronounced plateau in the frequency range tested and are significantly higher than the corresponding loss moduli (G'', data not shown) at day 0 for all degrees of alginate oxidation (Fig. 3A). As the actual oxidation of the alginate increased from 9% to 20%, the G' decreased. The OMA-44 hydrogels were too weak to measure their rheological properties.

To examine the correlation between polymer stiffness and polymer concentration in OMA hydrogels, G' of photocrosslinked OMA-14 hydrogels with different OMA concentrations were measured at day 0 (Fig. 3B). G' of OMA-14 hydrogels increased with increasing OMA concentration from 2 to 8 w/v %, and the values were independent of frequency.

To examine the correlation between mechanical property changes and degradation, dynamic mechanical analysis was also performed on the OMA-9 hydrogels during the degradation study to determine their storage moduli. As shown in Fig. 3C (2 w/v %) and 3D (4 w/v %), the storage moduli (G') of both 2 and 4 w/v % of OMA-9 hydrogels decreased during the course of degradation and were independent of frequency. All OMA-14 and OMA-20 hydrogels were too weak to measure their rheological property changes over time.

3.4. Cytotoxicity tests of OMA macromer and photocrosslinked hydrogel

The potential cytotoxicities of OMA macromers and photocrosslinked OMA hydrogels were evaluated by measuring the mitochondrial metabolic activity of hBMMSCs cultured on tissue culture plastic in the presence of the biomaterial using a standard MTS assay. The cell viability was calculated by normalizing the absorbance of samples at 490 nm to that of the control without any macromer or insert in the medium. The viability of cells cultured in the presence of OMA macromers and photocrosslinked hydrogels decreased after 48 h culture as the oxidation level increased (Fig. 4). There was no significant difference in cell viability between cells + insert group and OMA-9 macromer or photocrosslinked OMA-9 hydrogel groups, and between photocrosslinked OMA-9 and OMA-14 hydrogels.

3.5. hBMMSC attachment and morphology on OMA hydrogel surface

hBMMSCs were seeded onto the surface of photocrosslinked OMA hydrogels to evaluate if the degree of oxidation would affect cell adhesion and spreading. hBMMSCs adhered to the surfaces of photocrosslinked OMA hydrogels after 4 h of incubation (Fig. 5), and the number of adhered hBMMSCs on the OMA hydrogels increased as the hydrogel concentration increased (Fig. 5B). The number of adhered hBMMSCs on the 4 w/v % of OMA-20 hydrogel was significantly less than that on 4 w/v % of OMA-9 and OMA-14 hydrogels. The number of adhered hBMMSCs was similar on all three types hydrogels at 2 and 8 w/v %. OMA-44 hydrogels were completely degraded after 4 h of incubation.

The morphology of hBMMSCs on the photocrosslinked OMA hydrogel was also examined by fluorescence staining with a Live/Dead assay at day 7 (Fig. 5C). The fluorescence photomicrographs show that almost all of hBMMSCs cultured on 2 and 4 w/v % of OMA hydrogels displayed a rounded morphology. In contrast, most of hBMMSCs cultured on the 8 w/v % of OMA hydrogels were observed to spread at day 7. OMA-20 hydrogels were completely degraded after 7 days of culture.

3.6. hMSC encapsulation

hBMMSCs or hADSCs were photoencapsulated within OMA hydrogels. The viability of the photoencapsulated hMSCs in the OMA hydrogels was evaluated by Live/Dead assay to examine cell survival during the photocrosslinking process and in culture. High cell viability

was observed throughout all alginate hydrogel compositions for 4 weeks (Fig. 6A and B) using the Live/Dead assay. Additionally, the photoencapsulated hMSCs spread and proliferated in the OMA hydrogels at lower hydrogel concentrations. All OMA-20, and OMA-14 at 2 and 4 w/v % hydrogels were completely degraded within 1 week.

The DNA content of hMSCs in OMA-9 at 2 w/v % hydrogels was significantly greater than that of the other hydrogels at 2 and 4 weeks, and significantly increased over time in both hMSCs (Fig. 6C and D). After 4 weeks of culture, the DNA contents of hBMMSCs photoencapsulated in the OMA-9 at 4 w/v % and OMA-14 at 8 w/v % hydrogels significantly increased (Fig. 6C). The DNA content of hADSCs in OMA-9 at 4 w/v % hydrogels also increased significantly over time (Fig. 6D).

4. Discussion

In this study, we developed photocrosslinked alginate hydrogels with an increased range of biodegradation rates for more rapid in vivo biodegradation, and controlled mechanical properties and swelling for tissue engineering applications. Hydrogels, which support and regulate cell adhesion, migration, proliferation, and differentiation, play an important role in tissue engineering [18]. Hydrogels should degrade into non-toxic byproducts after fulfilling their functions. The coordination of hydrogel degradation rate and new tissue formation rate is an essential design criterion to be considered [6,19]. In addition, the mechanical properties of materials can strongly affect cell function, and thus control of this physical parameter in hydrogels may be quite valuable for their use in tissue engineering applications [20–22]. The results of this study demonstrated that changing the degree of alginate oxidation could allow for enhanced control over the swelling behavior, stiffness, and degradation rate of photocrosslinked alginate hydrogels (Figs. 2 and 3).

Previously, we prepared photocrosslinked alginate hydrogels with tunable physical properties [1], cell adhesivity [2], and growth factor delivery capacity [3]. The photocrosslinked alginate hydrogels are promising as cell carriers for tissue engineering applications since macromer solutions containing cells can be minimally invasively injected into a target tissue defect and undergo in situ gelation [1,2]. However, while altering the degree of alginate methacrylation regulates the number of ester bonds in the alginate crosslinks available for potential hydrolysis, the degradation rate of photocrosslinked alginate hydrogels is slower in physiological environments compared to in pure water due to the presence of positively charged cations (e.g., calcium and magnesium). The cations in physiologic solutions may decrease the osmotic pressure of hydrogel [23] and induce a small degree of ionic crosslinking resulting in decreased hydrogel swelling, and may act to delay degradation of alginate hydrogels. In addition, in some in vivo environments, there may be less aqueous solution surrounding the hydrogels compared to in vitro, thus decreasing the rate of hydrolytic degradation of the ester groups in the hydrogel crosslinks. Previously, methacrylated alginate has been oxidized but it was used as a biodegradable polymer crosslinker to make photocrosslinked poly(ethylene glycol) and poly(N-hydryoxymethyl acrylamide) hydrogels, not as the sole hydrogel macromer [12]. In this study, we also oxidized alginate prior to methacrylation to change the uronate residue conformations to an open-chain adduct, which would be more prone to hydrolysis [10], to increase the biodegradation rate of photocrosslinked alginate hydrogels. In our previous report, photocrosslinked hydrogels formed with alginate (2 w/v %) that had not been oxidized showed relatively slow degradation in DMEM [2,3], losing approximately 20% of their mass by eight weeks. Here, the photocrosslinked OMA-9 (2 w/v %) and OMA-14 (2 w/v %) hydrogels lost 73.9% and 100.0%, respectively, of their mass in DMEM by 3 weeks, indicating that degradation of the hydrogels could be dramatically increased by oxidation of the alginate. We have shown that the swelling behavior, degradation profiles, and

rheological properties of photocrosslinked hydrogels formed with OMAs can be further tuned by varying the alginate degree of oxidation and concentration in the hydrogels.

Hydrogels and their degradation products must be cytocompatible for tissue engineering applications [20]. As determined by the MTS assay, the viability of hBMMSCs in monolayer culture following exposure to OMA macromers and photocrosslinked OMA hydrogels indicates the cytocompatible and non-toxic nature of biomaterial. hBMMSC viabilities in the presence of OMAs or photocrosslinked OMA hydrogels were at least 75.9% at the highest oxidation levels and as high as 96.9% for the OMA-9 compared to controls, suggesting that the photocrosslinked alginate hydrogels and degradation products are relatively non-toxic.

Photocrosslinked non-oxidized alginate hydrogels present an environment absent of cell adhesion molecules and they exhibit minimal cell adhesion [1,2]. When the hBMMSCs were seeded on top of the photocrosslinked non-oxidized alginate hydrogels, few cells (2.7%) were able to adhere after 4 h and those that did remained rounded through 5 days (data not shown). In contrast, a larger quantity of hBMMSCs (at least 10.6%) adhered to the surface of the photocrosslinked OMA-9 and OMA-14 hydrogels by 4 h and they exhibited substantial spreading by 7 days on the hydrogels prepared with a higher concentration of OMA. It is likely that free aldehydes of photocrosslinked OMA hydrogels bind to amines present on cell surface proteins or extracellular matrix [24]. These results suggest that the photocrosslinked OMA hydrogels can promote enhanced cell adhesion and spreading compared to those prepared with alginate that has not been oxidized.

Photocrosslinked OMA hydrogels provide many advantages over calcium crosslinked alginate hydrogels or photocrosslinked non-oxidized alginate hydrogels. The photoinitiated reaction permits rapid polymerization rates in cytocompatible conditions, as evidence by high cell viability of encapsulated hMSCs that was observed throughout all OMA hydrogels over the course of 28 days cultured in vitro, indicating that the whole system, including the photoencapsulation process, the OMA hydrogels themselves, and their degradation products, is cytocompatible. Additionally, the photoencapsulated hMSCs spread and proliferated in the OMA hydrogels at lower hydrogel concentrations (Fig. 6). When the proliferation of photoencapsulated hMSCs in the OMA hydrogels was examined by DNA content as a function of culture time, the DNA content within the photocrosslinked OMA hydrogels (2 and 4 w/v %) was significantly increased at 4 weeks (Fig. 6B). This may be explained by the fact that the higher swelling and degradation of hydrogels provided increased space to enhance cell spreading, migration and proliferation, and these physical changes may allow for improved mass transfer of oxygen and nutrients, which are essential for cell survival and proliferation. This finding also corroborates other reports where biodegradable hydrogels enhanced the proliferation of encapsulated cells in hydrogel [25,26].

5. Conclusions

In this study, we have engineered a photocrosslinked and biodegradable hydrogel using OMA with controllable swelling ratio, stiffness, and degradation rates. These physical properties could be tuned by varying the degree of alginate oxidation and weight concentration of OMA, in addition to varying the degree of alginate methacrylation. The photocrosslinked OMA hydrogels exhibited relatively low cytotoxicity and excellent cytocompatibility. hMSCs could be easily encapsulated with the OMA hydrogels via suspension followed by in situ photopolymerization in culture media solutions of OMA, remained viable, and proliferated for 4 weeks in some formulations. The photocrosslinked OMA hydrogels developed in this study may find great utility in tissue engineering, including applications in stem cell transplantation and controlled bioactive factor delivery.

Acknowledgments

The authors thank Dr. Arnold Caplan's Skeletal Research Center Mesenchymal Stem Cell facility, especially Dr. Donald Lennon and Ms. Margie Harris, for providing the hBMMSCs, and Dr. Jeffrey Gimble, Dr. Xiying Wu, and Ms. Forum Shah at the Pennington Biomedical Research Center's Stem Cell Biology Laboratory for providing the hADSC. Funding support is gratefully acknowledged from the Musculoskeletal Transplant Foundation, Biomedical Research and Technology Transfer Grants 08-081 and 09–071 from the Ohio Department of Development (EA) and a New Scholar in Aging grant from the Ellison Medical Foundation (EA).

References

1. Jeon O, Bouhadir KH, Mansour JM, Alsberg E. Photocrosslinked alginate hydrogels with tunable biodegradation rates and mechanical properties. Biomaterials. 2009; 30:2724–34. [PubMed: 19201462]
2. Jeon O, Powell C, Ahmed SM, Alsberg E. Biodegradable, photocrosslinked alginate hydrogels with independently tailorable physical properties and cell adhesivity. Tissue Eng Part A. 2010; 16:2915–25. [PubMed: 20486798]
3. Jeon O, Powell C, Solorio LD, Krebs MD, Alsberg E. Affinity-based growth factor delivery using biodegradable, photocrosslinked heparin-alginate hydrogels. J Control Release. 2011; 154:258–66. [PubMed: 21745508]
4. Prang P, Muller R, Eljaouhari A, Heckmann K, Kunz W, Weber T, et al. The promotion of oriented axonal regrowth in the injured spinal cord by alginate-based anisotropic capillary hydrogels. Biomaterials. 2006; 27:3560–9. [PubMed: 16500703]
5. Read TA, Stensvaag V, Vindenes H, Ulvestad E, Bjerkvig R, Thorsen F. Cells encapsulated in alginate: a potential system for delivery of recombinant proteins to malignant brain tumours. Int J Dev Neurosci. 1999; 17:653–63. [PubMed: 10571425]
6. Alsberg E, Kong HJ, Hirano Y, Smith MK, Albeiruti A, Mooney DJ. Regulating bone formation via controlled scaffold degradation. J Dent Res. 2003; 82:903–8. [PubMed: 14578503]
7. Boontheekul T, Kong HJ, Mooney DJ. Controlling alginate gel degradation utilizing partial oxidation and bimodal molecular weight distribution. Biomaterials. 2005; 26:2455–65. [PubMed: 15585248]
8. Gomez CG, Rinaudo M, Villar MA. Oxidation of sodium alginate and characterization of the oxidized derivatives. Carbohyd Polym. 2007; 67:296–304.
9. Kong HJ, Kaigler D, Kim K, Mooney DJ. Controlling rigidity and degradation of alginate hydrogels via molecular weight distribution. Biomacromolecules. 2004; 5:1720–7. [PubMed: 15360280]
10. Bouhadir KH, Lee KY, Alsberg E, Damm KL, Anderson KW, Mooney DJ. Degradation of partially oxidized alginate and its potential application for tissue engineering. Biotechnol Prog. 2001; 17:945–50. [PubMed: 11587588]
11. Lee KY, Bouhadir KH, Mooney DJ. Evaluation of chain stiffness of partially oxidized polyguluronate. Biomacromolecules. 2002; 3:1129–34. [PubMed: 12425648]
12. Cha C, Kohmon RE, Kong H. Biodegradable polymer crosslinker: independent control of stiffness, toughness, and hydrogel degradation rate. Adv Funct Mater. 2009; 19:3056–62.
13. Balakrishnan B, Lesieur S, Labarre D, Jayakrishnan A. Periodate oxidation of sodium alginate in water and in ethanol-water mixture: a comparative study. Carbohyd Res. 2005; 340:1425–9.
14. Beamish JA, Zhu JM, Kottke-Marchant K, Marchant RE. The effects of monoacrylated poly(ethylene glycol) on the properties of poly(ethylene glycol) diacrylate hydrogels used for tissue engineering. J Biomed Mater Res Part A. 2010; 92A:441–50.
15. Lennon DP, Haynesworth SE, Bruder SP, Jaiswal N, Caplan AI. Human and animal mesenchymal progenitor cells from bone marrow: identification of serum for optimal selection and proliferation. In Vitro Cell Dev Biol-Anim. 1996; 32:602–11.
16. Haynesworth SE, Goshima J, Goldberg VM, Caplan AI. Characterization of cells with osteogenic potential from human marrow. Bone. 1992; 13:81–8. [PubMed: 1581112]
17. Estes BT, Diekman BO, Gimble JM, Guilak F. Isolation of adipose-derived stem cells and their induction to a chondrogenic phenotype. Nat Protoc. 2010; 5:1294–311. [PubMed: 20595958]

18. Jin, R.; Dijkstra, PJ. Hydrogels for tissue engineering applications. In: Park, K.; Okano, T., editors. Biomedical applications of hydrogels handbook. New York: Springer; 2010. p. 203-25.
19. Park JB. The use of hydrogels in bone-tissue engineering. Medicina Oral Patologia Oral Y Cirugia Bucal. 2011; 16:E115–8.
20. Nicodemus GD, Bryant SJ. Cell encapsulation in biodegradable hydrogels for tissue engineering applications. Tissue Eng Part B. 2008; 14:149–65.
21. Engler AJ, Sen S, Sweeney HL, Discher DE. Matrix elasticity directs stem cell lineage specification. Cell. 2006; 126:677–89. [PubMed: 16923388]
22. Khatiwala CB, Peyton SR, Putnam AJ. Intrinsic mechanical properties of the extracellular matrix affect the behavior of pre-osteoblastic MC3T3-E1 cells. Am J Physiol-Cell Physiol. 2006; 290:C1640–50. [PubMed: 16407416]
23. Bin Imran A, Seki T, Takeoka Y. Recent advances in hydrogels in terms of fast stimuli responsiveness and superior mechanical performance. Polym J. 2010; 42:839–51.
24. Shazly TM, Baker AB, Naber JR, Bon A, Van Vliet KJ, Edelman ER. Augmentation of postswelling surgical sealant potential of adhesive hydrogels. J Biomed Mater Res Part A. 2010; 95A:1159–69.
25. Nguyen KT, West JL. Photopolymerizable hydrogels for tissue engineering applications. Biomaterials. 2002; 23:4307–14. [PubMed: 12219820]
26. Bryant SJ, Cuy JL, Hauch KD, Ratner BD. Photo-patterning of porous hydrogels for tissue engineering. Biomaterials. 2007; 28:2978–86. [PubMed: 17397918]

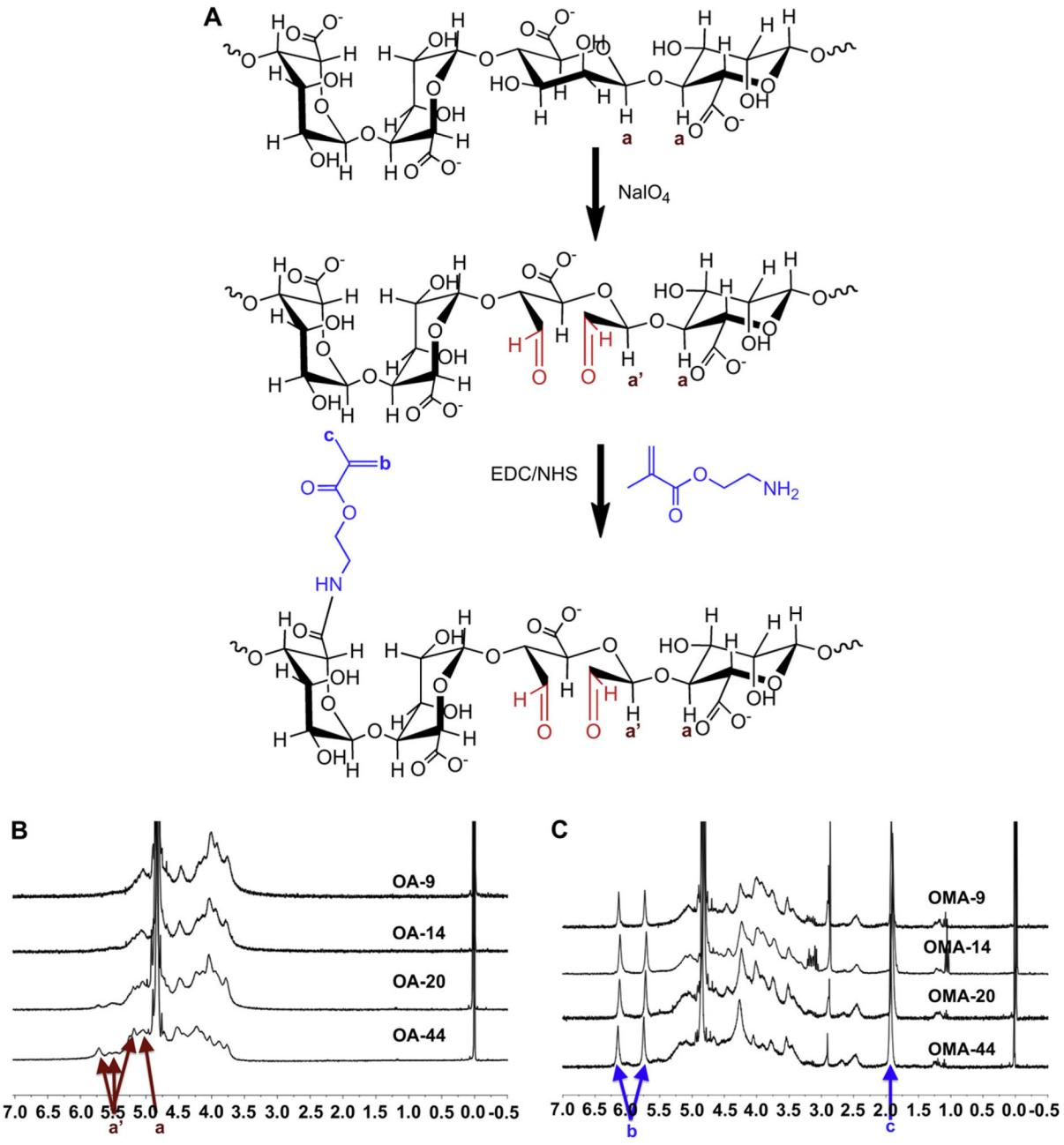

Fig. 1.

(A) Schematic illustration for preparation of the OMA and ^{1}H NMR spectra of (B) OAs and (C) OMAs with various degrees of oxidation in D_2O.

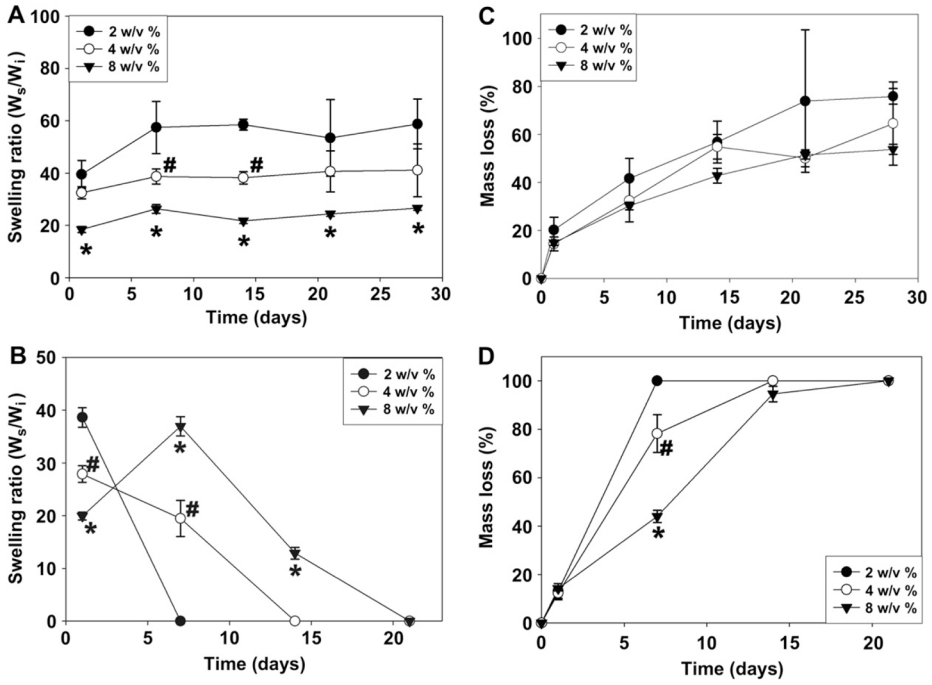

Fig. 2.

Swelling ratios of photocrosslinked (A) OMA-9 and (B) OMA-14 hydrogels and mass loss of (C) OMA-9 and (D) OMA-14 hydrogels in DMEM over time. Values represent mean ± standard deviation ($N = 3$). *$p < 0.05$ compared with 2 and 4 w/v %, and #$p < 0.05$ compared with 2 w/v %.

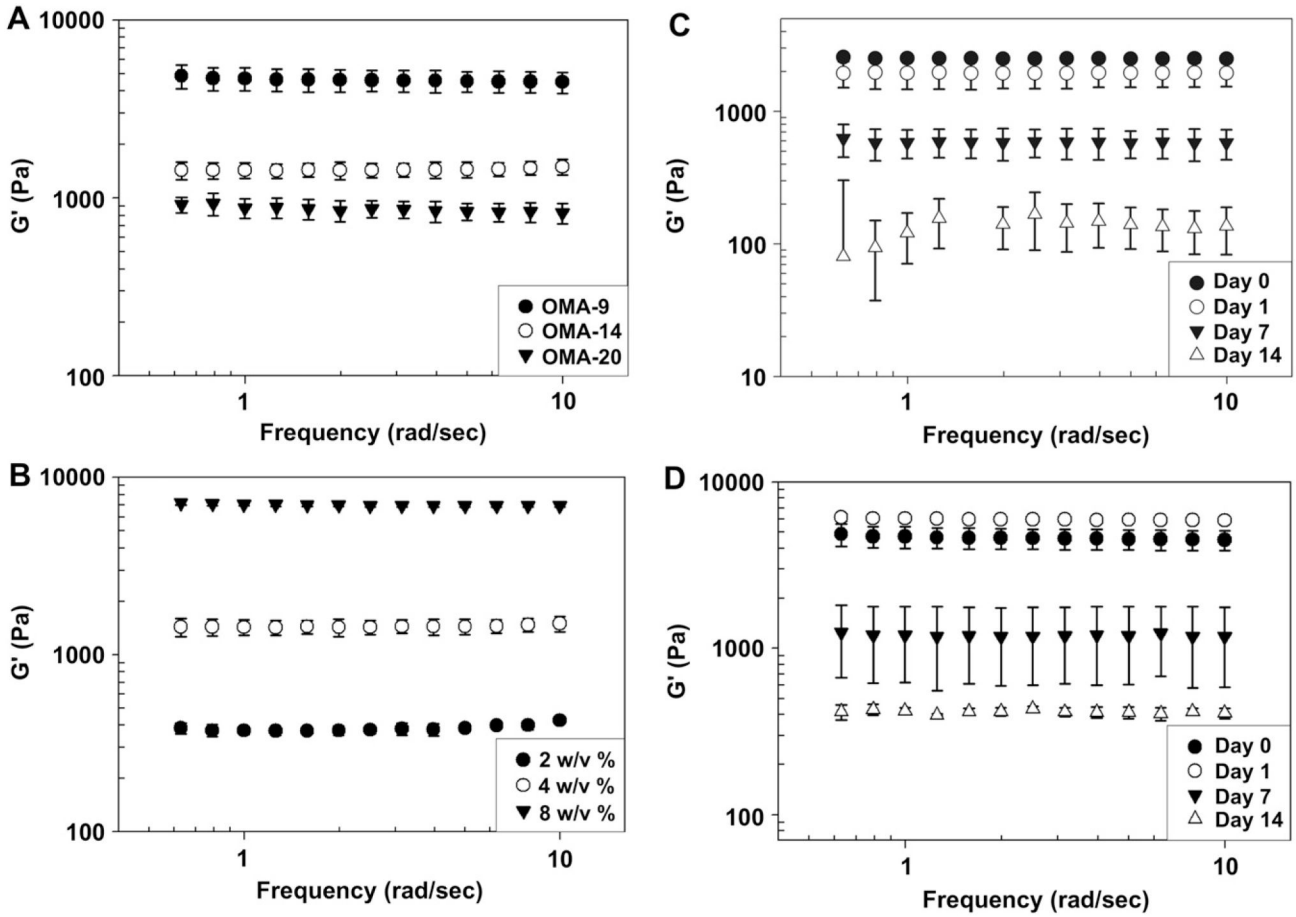

Fig. 3.

Characterization of shear elastic moduli of photocrosslinked OMA hydrogels by rheological measurements. (A) Storage moduli (G′) of photocrosslinked OMA (4 w/v %) hydrogels during frequency sweep analysis at day 0. (B) G′ of photocrosslinked OMA-14 hydrogels with three different weight percentages of macromers comprising the hydrogels at day 0. G′ changes of OMA-9 hydrogels at (C) 2 and (D) 4 w/v % during degradation. Values represent mean ± standard deviation ($N = 3$).

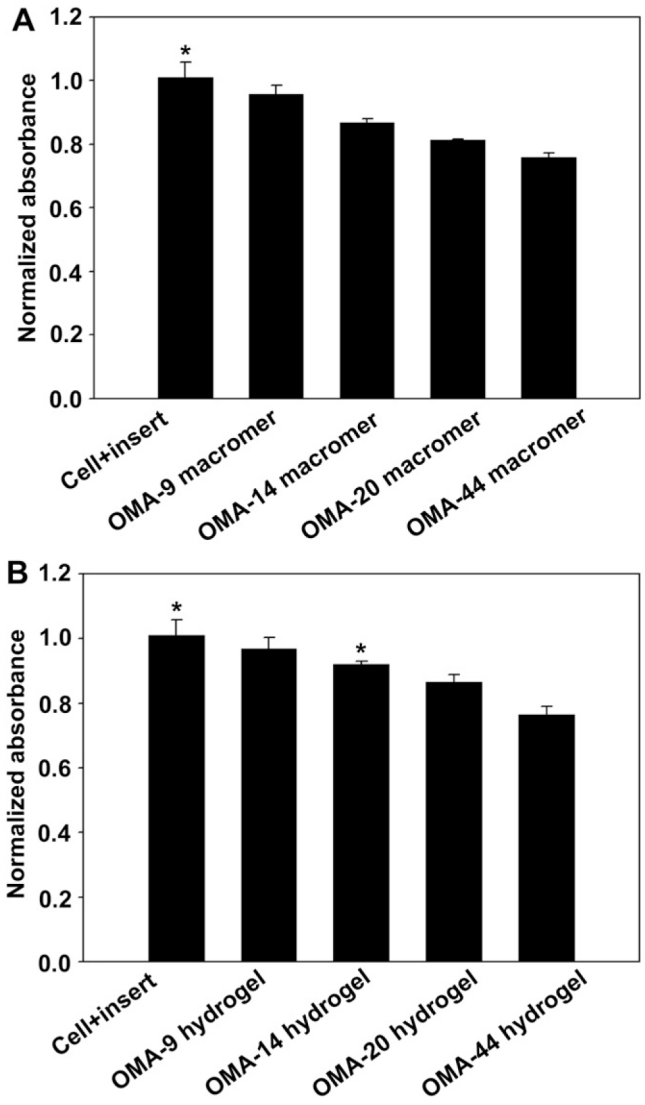

Fig. 4.

Cytotoxicity of (A) OMA macromers and (B) photocrosslinked OMA hydrogels on hBMMSCs after 48 h as quantified by an MTS assay and normalized by the absorbance of samples at 490 nm to that of the control without any macromer or insert in the medium. Values represent mean ± standard deviation ($N = 3$) *$p > 0.05$ compared with OMA-9.

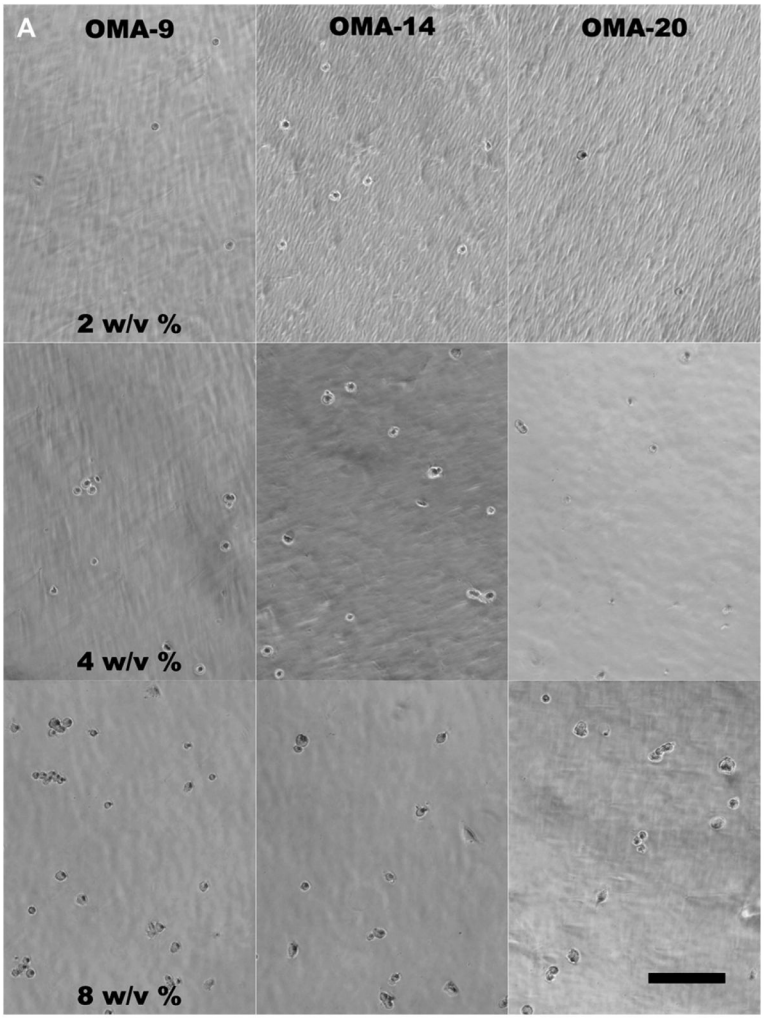

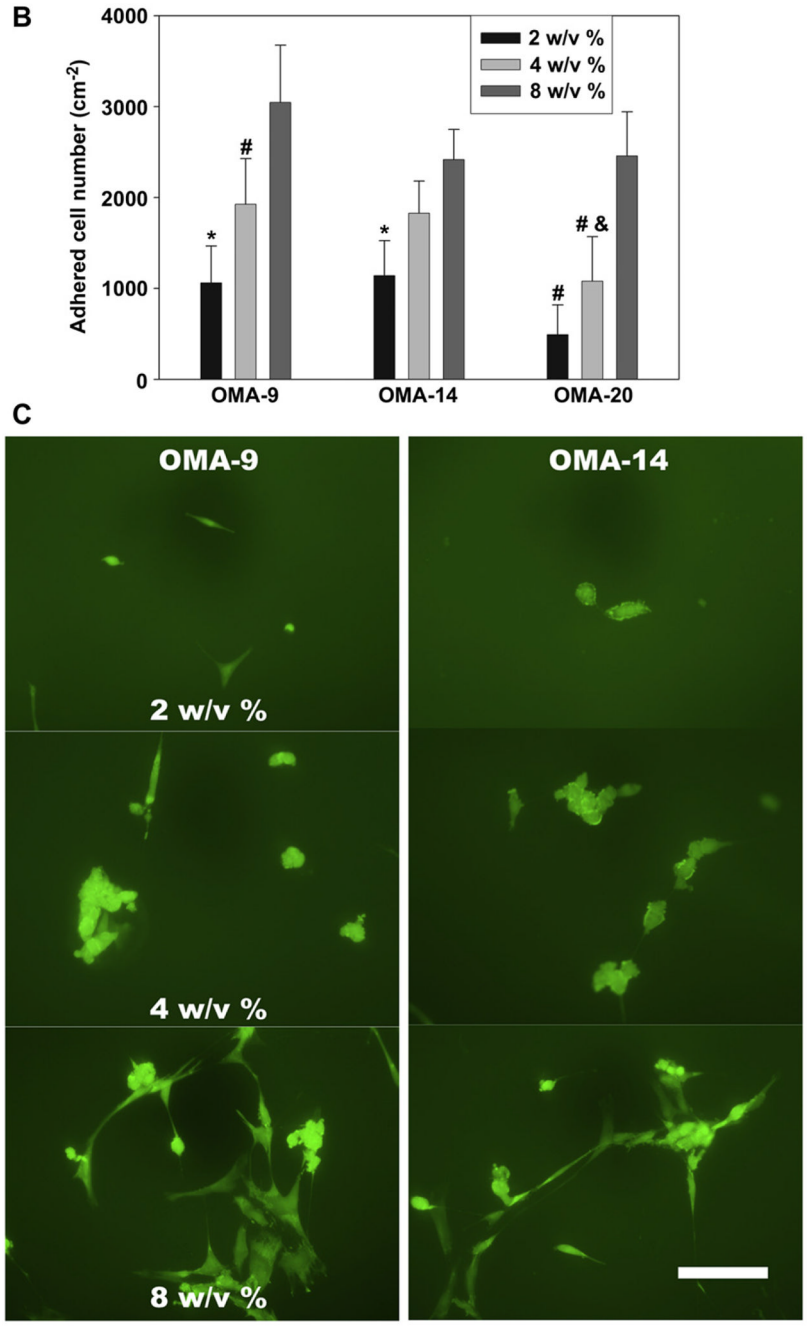

Fig. 5.

Light photomicrographs of hBMMSCs after 4 h culture on (A) the photocrosslinked OMA hydrogels, and (B) quantification of adherent cell number. (C) Fluorescence photomicrographs of live (FDA, green) and dead (EB, orange-red) hBMMSCs cultured on the surface of photocrosslinked OMA hydrogels in vitro at 7 days. The scale bar indicates 200 μm and all photographs were taken at the same magnification. Values represent mean ± standard deviation ($N = 3$). *$p < 0.05$ compared to 4 and 8 w/v % at a specific OMA hydrogel. $^{\#}p < 0.05$ compared to 8 w/v % at a specific OMA hydrogel. $^{\&}p < 0.05$ compared to OMA-9 (4 w/v %) and OMA-14 (4 w/v %). (For interpretation of the references to color in this figure legend, the reader is referred to the web version of this article.)

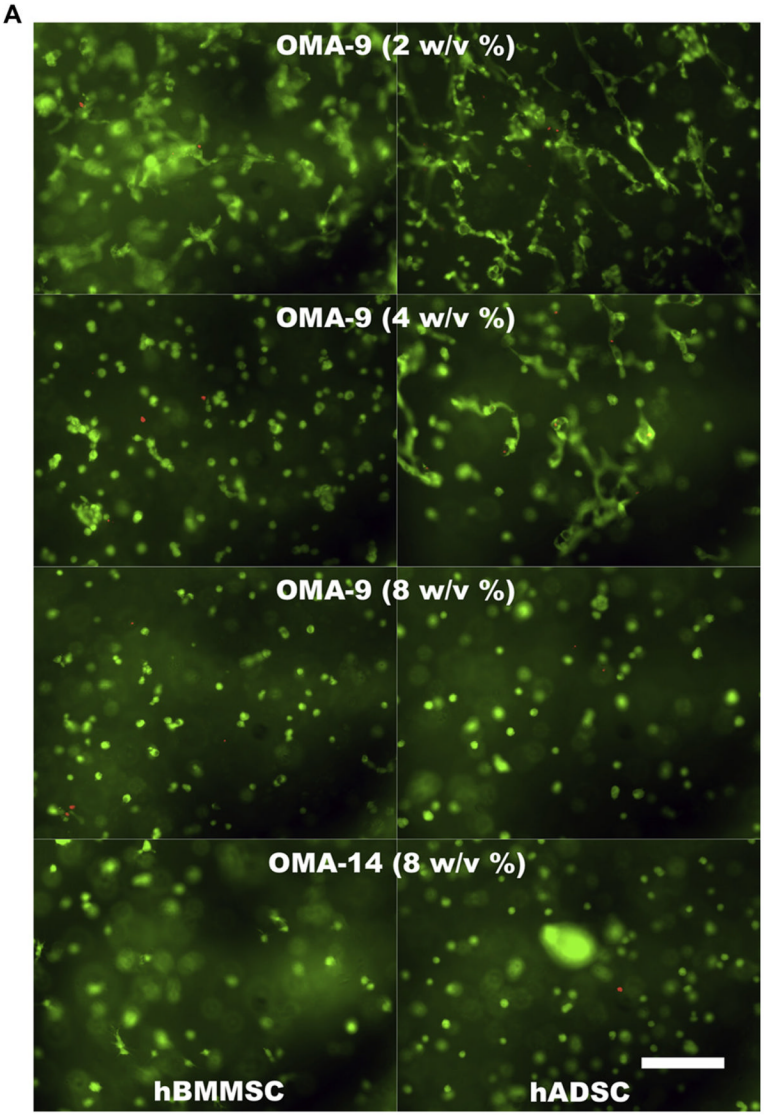

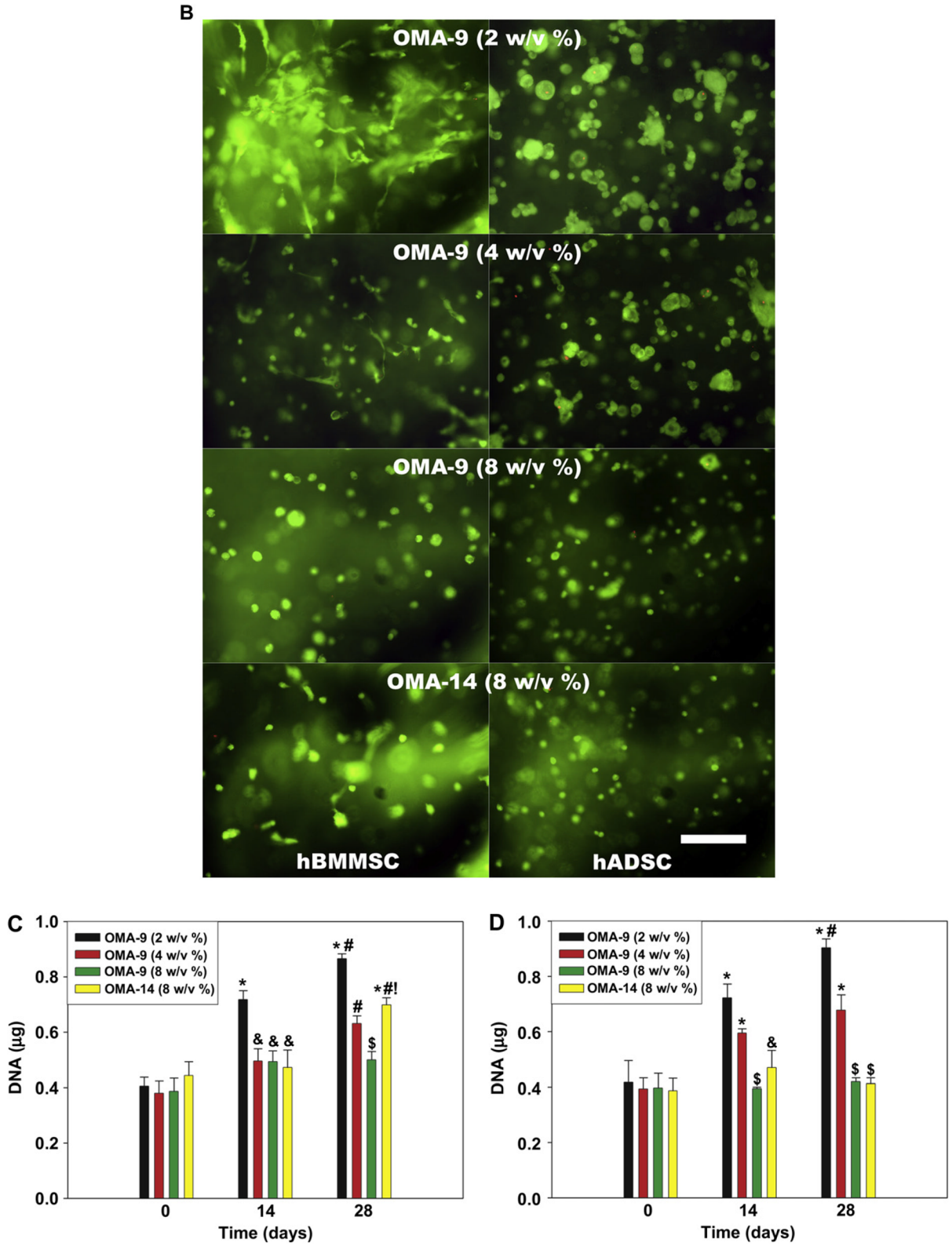

Fig. 6.

Fluorescence photomicrographs of live (FDA, green) and dead (EB, orange-red) hMSCs cultured in vitro after (A) 14 and (B) 28 days in the photocrosslinked OMA hydrogels, and quantification of DNA content in the (C) hBMMSC and (D) hADSC/hydrogel constructs. The scale bar indicates 200 μm and all photographs were taken at the same magnification. Values represent mean ± standard deviation ($N = 3$). $^{*}p < 0.05$ compared to day 0 at a same group. $^{\#}p < 0.05$ compared to day 14 at a same group. $^{\&}p < 0.05$ compared to OMA-9 (2 w/v %) at a specific time point. $^{\$}p < 0.05$ compared to OMA-9 (2 and 4 w/v %) at a specific time point. $^{!}p < 0.05$ compared to OMA-9 (2 and 8 w/v %) at a specific time point. (For interpretation of the references to color in this figure legend, the reader is referred to the web version of this article.)

Table 1

Oxidation efficiency (%), actual oxidation (%), weight average molecular weight of OMAs, and elastic modulus of photocrosslinked alginate hydrogels.

Code	Theoretical oxidation (%)[a]	Oxidation efficiency (%)[b]	Actual oxidation (%)[b]	Weight average molecular weight (Da)[c]	Storage modulus (Pa)[d]
OMA-9	10	90	9	74,970	4693 ± 691
OMA-14	17.5	80	14	35,230	1431 ± 145
OMA-20	25	80	20	17,820	879 ± 112
OMA-44	50	88	44	13,200	_[e]

[a] Theoretical oxidation of uronic acid units was calculated based on the mass of alginate in 1(w/v %) alginate solution and molecular weight of the repeat unit (M_0 = 198).

[b] Oxidation efficiency and actual oxidation were calculated from ^{1}H NMR data.

[c] The molecular weight of OMA was measured by GPC.

[d] Elastic modulus was obtained at 1 rad/s frequency from rheometer measurement.

[e] It was not possible to perform a rheometer measurement on the OMA-44.